Nanoscale

RSC Publishing

PAPER

View Article Online
View Journal | View Issue

Published on 08 August 2013. Downloaded by Korea Institute of Science and Technology / KIST on 02/10/2013 09:11:20.

Cite this: Nanoscale, 2013, 5, 10014

# Hierarchical structures of AlOOH nanoflakes nested on Si nanopillars with anti-reflectance and superhydrophobicity

Eusun Yu,[ab] Heon Ju Lee,[b] Tae-Jun Ko,[ab] Seong Jin Kim,[b] Kwang-Ryeol Lee,[b] Kyu Hwan Oh[a] and Myoung-Woon Moon*[b]

Received 9th May 2013
Accepted 4th August 2013

DOI: 10.1039/c3nr02395h

www.rsc.org/nanoscale

A novel method to fabricate ultra-low reflective Si surfaces with nanoscale hierarchical structures is developed by the combination of AlOOH or boehmite nanoflakes nested on plasma-etched Si nanopillars. Using $CF_4$ plasma etching, Si surfaces are nanostructured with pillar-like structures by selective etching with self-masking by fluorocarbon residues. AlOOH nanoflakes are formed by Al thin film coating with various thicknesses and subsequent immersion in boiling water, which induces the formation of nanoscale flakes through the hydrolysis reaction. AlOOH nanoflakes are formed on Si nanopillared surfaces for hierarchical structures, which are coated with a low-surface-energy material, resulting in a higher water wetting angle of over 150° and a very low contact angle hysteresis of less than 5°, and implying a self-cleaning surface. Reflectance reduced to 5.18% on average on hierarchical nanostructures in comparison to 9.63% on the Si nanopillar surfaces only. We found that Si nanopillars reduced reflection for wavelengths ranging from 200 to 1200 nm while AlOOH nanoflakes reduced reflection for wavelengths longer than 600 nm.

## 1 Introduction

Continuous efforts have been made to the development of ultra-low- or anti-reflective superhydrophobic surfaces for use in solar cell panels or detecting devices to increase cell performance and durability *via* self-cleaning under harsh environments.[1,2] To enhance solar cell performance, studies have addressed several issues, ranging from the high absorption rate of sunlight to the conversion efficiency of light into electrical energy. High-energy sunlight absorption can be achieved by reducing scattering or reflection on the surfaces by adopting efficiently designed structures in nature such as moth-eye micro/nanoscale pillar structures. It is known that the natural designs achieve anti-reflection by using well-aligned arrays of ripples for the systematic reduction of reflection and improvement of transmission, allowing insects such as moths and butterflies to live in low-intensity light available in the night time. Especially, the tapered cross-sectional profiles of such anti-reflective structures increase the refractive index difference between air and the surface feature, maximizing light transmission.[3–5]

Inspired by moth-eye structures, several studies have developed low-reflective surfaces on various materials such as semiconductors, polymers, diamonds, or metals using e-beam evaporation, chemical vapor deposition, sputtering, plasma or reactive ion etching (RIE), and sol–gel or hydrothermal techniques.[6–8] In particular, Si surfaces with nanostructures known as nanograss made by RIE or nanoimprinting have been reported to have very low reflectance (0.8%) for 400 to 800 nm light. However, these methods suffer from high cost, complex fabrication, and the use of toxic solutions such as HF or HCl to form the Si nanostructures. Furthermore, to improve the absorption rate of light, several studies have reported multi-scale roughness by forming ZnO nanostructures on micro-structured silicon using continuous solution methods.[9]

Superhydrophobic surfaces are crucial for maintaining the durability of solar cell panels, which should gather sunlight without loss through reflectance under harsh environments such as deserts, and thus require self-cleaning or easy cleaning procedures. Moth-eye surfaces have also achieved self-cleaning using the high fraction of air trapped between textured arrays.[10,11] Hydrophobic or superhydrophobic surfaces are achieved by applying coatings with low surface energy on textured surfaces, which usually mimic micro-/nano- or hybrid structures such as a lotus leaf, which has a high water contact angle (CA) and low contact angle hysteresis (CAH).[12] When a water droplet is placed on a lotus leaf, it forms a nearly perfect spherical shape that rolls off and cleans the contaminated surfaces.[13]

Herein, we have developed a novel method to fabricate ultra-low reflective and superhydrophobic Si surfaces having hierarchical structures using aluminum oxide hydroxide (or AlOOH)

[a]Department of Materials Science and Engineering, Seoul National University, 1 Gwanak-ro, Gwanak-gu, Seoul (151-742), Republic of Korea

[b]Institute for Multidisciplinary Convergence of Matter, Korea Institute of Science and Technology, Seoul (136-791), Republic of Korea. E-mail: mwmoon@kist.re.kr



This journal is © The Royal Society of Chemistry 2013

Published on 08 August 2013. Downloaded by Korea Institute of Science and Technology / KIST on 02/10/2013 09:11:20.

nanoflakes nested on plasma-etched Si nanopillars. This method allows the non-toxic, fast, and room-temperature fabrication of dual-scale hierarchical surfaces on Si. Nanopillared Si surfaces and AlOOH nanoflakes fabricated individually provide anti-reflection due to the high nanoscale roughness and superhydrophobicity by coating with low-surface-energy materials, respectively.[14] However, the combination of these two structures improves hydrophobicity and anti-reflectance. AlOOH nanoflakes are formed by Al thin film coating with various thicknesses and subsequent immersion in boiling water, which induces the formation of nanoscale flakes. AlOOH nanoflakes are formed on Si nanopillared surfaces for the fabrication of hierarchical structures as shown in Fig. 1.

$SiO_x$-containing DLC ($SiO_x$–DLC) films are coated *via* plasma polymerization of a hexamethyldisiloxane (HMDSO) vapor on prepared samples to increase hydrophobicity. Water CA and CAH measurements are performed to characterize the robustness of the superhydrophobic surfaces for wettability. The optical reflectance as a function of surface structure is analyzed by UV-Vis spectroscopy.

## 2 Experimental

The overall procedure for the fabrication of hierarchical nanostructures on Si (100) is shown in Fig. 1. Detailed conditions for the formation and characterization of the structures are provided below.

### 2.1 Sample preparation

Si (100) surfaces with nanoscale pillars are formed by the $CF_4$ plasma etching of flat bare Si wafers. Si wafers are etched to form nanopillars through a reactive ion etching using a radio frequency (r.f.) glow discharge of $CF_4$ gas at 30 mTorr and −600 V bias voltage.[15] This simple etching procedure produced nanopillars on the Si surface by selective etching. It is known that $CF_4$ plasma-treated Si surfaces have local fluorocarbon clusters formed from the $CF_4$ plasma and turned into a self-mask against fluorine reaction. However, Si surfaces without fluorocarbon clusters are preferred for etching of Si with the F atoms, which have high reactivity toward Si.[16] A $CF_4$ plasma

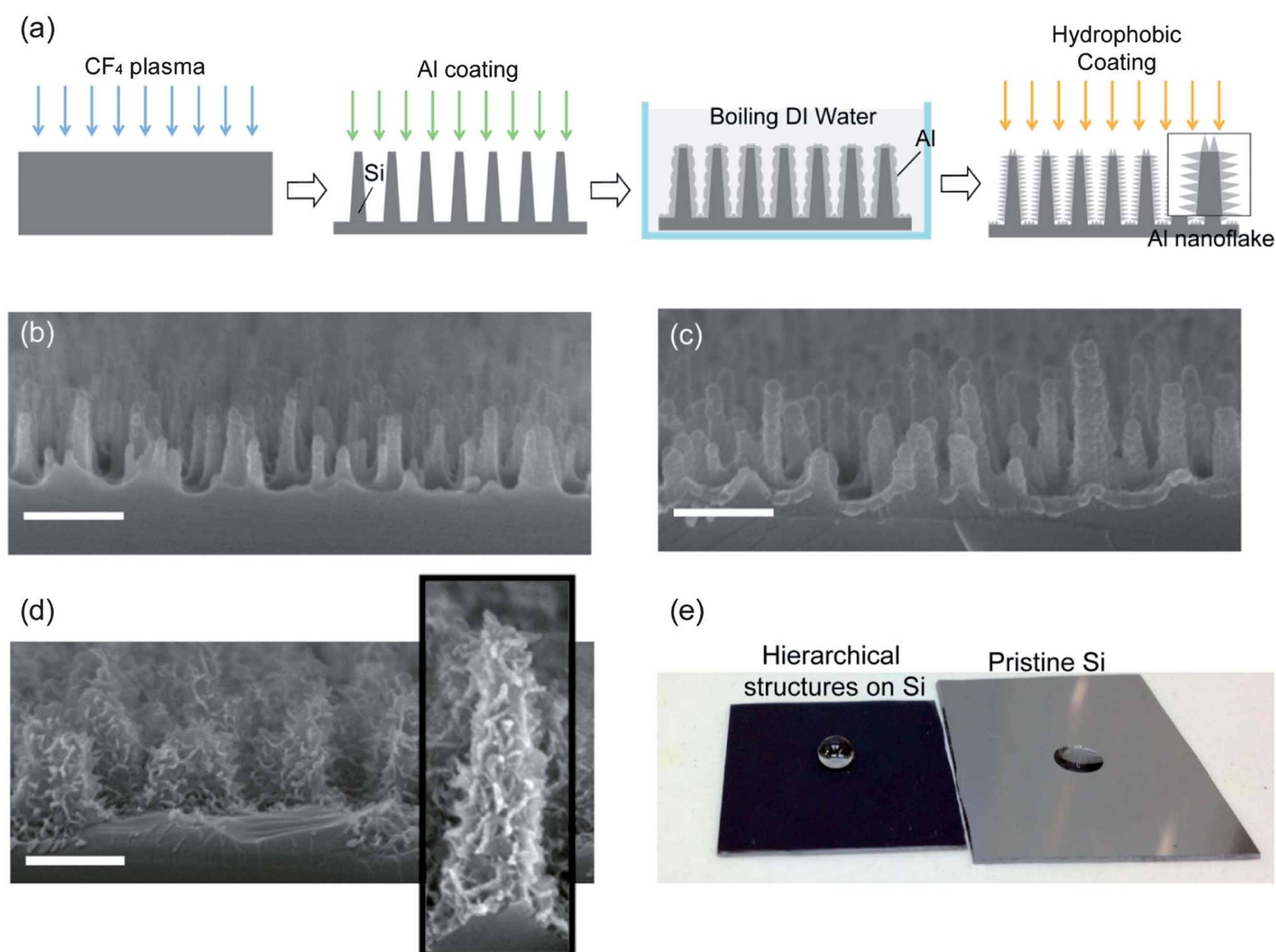


**Fig. 1** (a) Schematic for the fabrication of hierarchical nanostructures. (b) Si nanopillars are formed by $CF_4$ plasma etching for 60 min. (c) Si nanopillar surfaces are coated with 10 nm thickness Al by e-beam evaporation. (d) Al-coated Si surfaces are immersed in boiling water at a temperature of above 100 °C for 10 min, resulting in a hierarchical structure of Si nanopillars covered by AlOOH nanoflakes. Representative images taken by SEM have the same magnification. The scale bar is 500 nm. (e) Si surfaces with hierarchical nanostructures turned black and superhydrophobic. The width of the Si plate is 2 cm.

treatment duration ranging from 30–90 min is chosen to yield various surface roughnesses and aspect ratios.[15] This is defined as the ratio of pillar height to pillar diameter. The pillar height is controlled from 500 to 1500 nm, and the diameter is about 100 nm. Al hydroxide nanoflakes are fabricated by Al thin film coating with e-beam evaporation and subsequent boiling-water immersion. The thickness of the Al coating on flat and nanostructured Si surfaces is varied from 10 to 50 nm. Al coated samples are immersed in boiling water for 10 min, which resulted in the formation of Al hydroxide nanostructures.

Published on 08 August 2013. Downloaded by Korea Institute of Science and Technology / KIST on 02/10/2013 09:11:20.

### 2.2 Hydrophobic coating

The $SiO_x$–DLC film is coated on the surfaces using a HMDSO precursor *via* r.f. plasma-assisted chemical vapor deposition (PACVD). The $SiO_x$–DLC film from the plasma polymerization of HMDSO is chosen to increase the surface hydrophobicity due to a low surface energy of 24.2 mN $m^{-1}$. The film is known to have good mechanical performance in terms of wear resistance, hardness, and controllable coating thickness.[17] The bias voltage and working pressure are −400 V and 10 mTorr for 5 s, respectively, which resulted in a static CA of 90° for the $SiO_x$–DLC films on flat surfaces. However, the CA is approximately equal to or greater than 160° on the nanostructured surfaces. The detailed process used in the fabrication of superhydrophobic surfaces is implemented from a previous study.[15]

### 2.3 Characterization

We characterized the wettability of the hierarchically nanostructured surfaces by measuring the CA and CAH of deionized (DI) water droplets. For these measurements, approximately 5 μL in volume water droplets with a radius of approximately 1 mm are gently deposited on the surfaces using a microsyringe. The advancing CA is measured by adding a DI water sessile drop (~5 μL) and the receding CA by the removal of water from a DI water sessile drop. The CAH is calculated as the difference between the advancing and receding CAs. All measurements are taken using a contact angle goniometer (Rame-Hart) in ambient air at 15 °C with a relative humidity of 20–35%.

The reported CAs are determined by averaging the measurements from five different spots on each sample.

The nanostructures on the surfaces are observed with a scanning electron microscope (SEM, Nova 600, FEI), and the crystalline phase of the surfaces is examined by X-ray diffraction measurement (XRD, Bruker, D8 Advanced). Compositional analysis is performed with an X-ray photoelectron spectroscope (XPS) to investigate the chemical change from the hydrolysis reaction before and after the boiling water treatment on the Al-coated Si surfaces. An Al Kα (1486.6 eV) X-ray source is used as the excitation source, and the anode is maintained at 250 W, 10 kV, and 27 mA at a chamber pressure of $2.67 \times 10^{-8}$ Pa with a beam spot size of 400 μm × 400 μm. The peak position is calibrated using the C1s peak at 284.6 eV. The UV-Vis measurements are performed in the wavelength range of 200–1200 nm using a spectrophotometer (Perkin-Elmer, Lambda 20) at room temperature. The spectra are recorded by taking air as a reference.

## 3 Results and discussion

Al oxide nanoflakes formed on the flat Si surfaces with Al thicknesses ranging from 10 to 50 nm. As the thickness of the coated Al film increased, the configuration varied from sharply linear to relatively wide nanoflakes, ranging from 100 to 200 nm in length (Fig. 2). After the boiling water immersion test, the thickness of the Al oxide layer with nanoflakes increased by 10 times compared with the as-deposited Al film (Fig. 2). Fig. 3 shows the characteristics of the various surface morphologies of

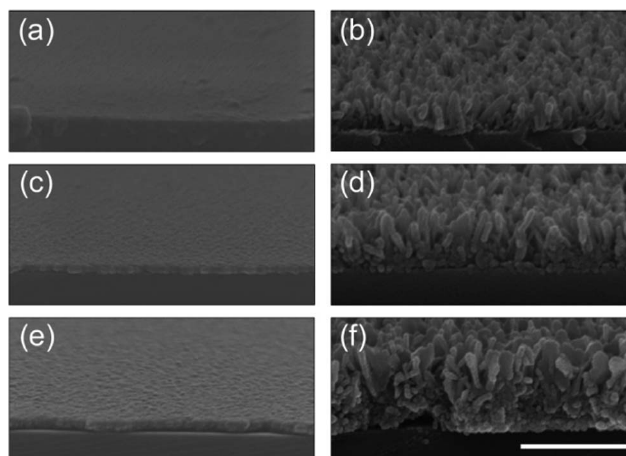


**Fig. 2** Cross-sectional SEM images of the Al-coated flat Si are measured with thicknesses of (a) 10 nm, (c) 30 nm, and (e) 50 nm at a 70° tilt-view. The Al-coated Si surfaces are coated by an e-beam evaporator and the corresponding images are shown after boiling water immersion for 10 min (b), (d), and (f), respectively. All images have the same magnification. The scale bar is 500 nm.

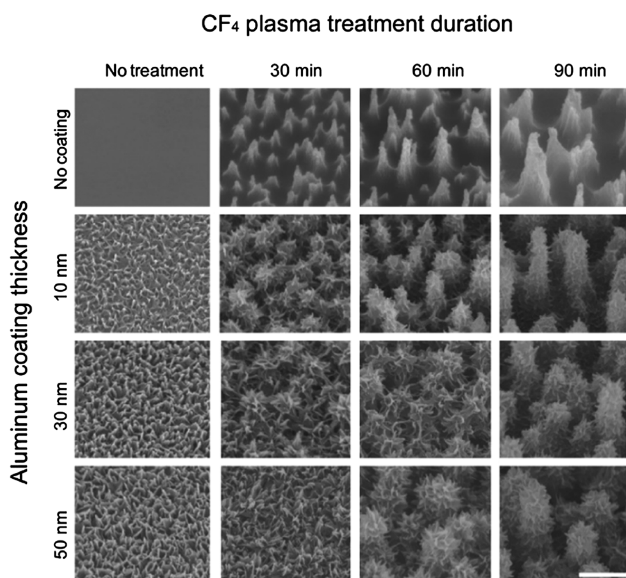


**Fig. 3** SEM images of single and hierarchical structures at a 30° tilt-view. Si nanopillars evolved with the plasma etching (from left to right). Al oxide nanoflakes formed on the Si surfaces with 0 nm, 10 nm, 30 nm and 50 nm coating thicknesses through a fixed hydrolysis duration of 10 min boiling water immersion. All images have the same magnification. The scale bar is 500 nm.

 This journal is © The Royal Society of Chemistry 2013

Published on 08 August 2013. Downloaded by Korea Institute of Science and Technology / KIST on 02/10/2013 09:11:20.

the Si surfaces: Si with pillars only and pillars decorated with or without Al oxide nanoflakes. The nanopillars have diameters of 100 to 150 nm and heights of 500 to 1500 nm with respect to the $CF_4$ plasma etching duration. Al oxide nanoflakes formed on top of the nanopillared Si, thereby resulting in a nanoscale hierarchical structure.

The Al oxide nanoflakes grew uniformly over the entire nanopillared Si, and the cover density increased with Al film thickness.

Some researchers reported that the reaction of Al in boiling water creates a porous nanostructure such as flakes or pseudo boehmite as confirmed by morphological observation and chemical analysis for water temperature and treatment duration.[18] It is known that in the immersion of Al in boiling or hot water, OH ions are sufficient to form AlOOH rather than $Al_2O_3$ at temperatures above 100 °C. After a brief boiling water treatment, AlOOH islands form and then spread over the Al surface. The islands achieve flake-like structures due to the bubbles

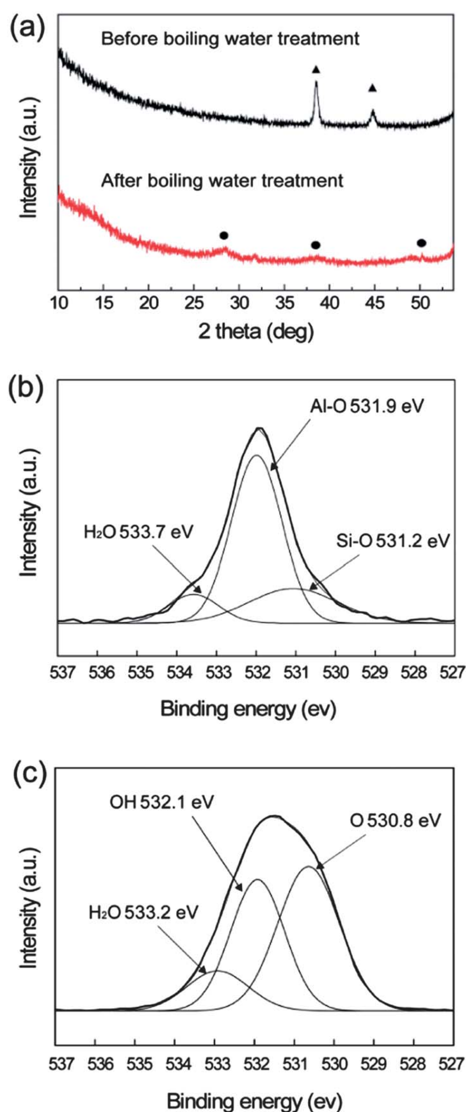


**Fig. 4** (a) XRD measurements before and after boiling water treatment and XPS spectra of Al coated surfaces (b) before and (c) after boiling water immersion.

bursting near the Al surface in boiling water.[19] To confirm this mechanism, the crystalline phase of Al oxide nanostructures is characterized by diffraction measurement (XRD) as shown in Fig. 4a. The Al-coated surface before boiling water treatment showed a peak related to the Al oxide phase induced by natural oxidation.

However, the surfaces after boiling water treatment revealed three characteristic peaks related to boehmite (AlOOH) with a broad and amorphous nature due to the thinness of the coated layer.[18,20]

XPS analysis of the Al surfaces with and without water immersion is performed to characterize the chemical change. The O1s XPS spectra with a range of 527–537 eV are used to distinguish the bonding information of AlOOH (Fig. 4b and c). The O1s peaks deconvoluted into two main peaks at 530.8 (O in AlO) and 531.9 (O in OH) and deconvoluted into two minor peaks related to a differential charge at 529.7 and 533.0 eV.[21] In the case of the O1s peak in AlOOH, both 530.8 and 531.9 eV peaks are dominant. However, only the 531.9 eV peak is dominant in the case of $Al_2O_3$ and $Al(OH)_3$. Studies showed that the boehmite structure is formed by the reaction between Al ions moving outwards from the Al bulk and hydroxyl ions formed on the external surface.[22,23] At a high temperature of 100 °C in water, the Al surface is attacked by bubbles and $Al^{3+}$ ions form, which combine with the abundance of $OH^-$ ions in boiling water and result in AlOOH boehmite. The final boehmite structure is amorphous due to the outward migration of cations and bubble attack.[24,25] This result indicates that the fabricated nanostructures formed on the surface consist of a boehmite phase of AlOOH.

The static CA and CAH of the sessile water droplets on the samples with various plasma durations with or without Al oxide nanoflakes are shown in Fig. 5. The flat Si surface with hydrophobic coating has a static contact angle of 90°, corresponding to the mild hydrophobic nature of a coated $SiO_x$–DLC film. The Si surfaces with nanopillars formed by different $CF_4$ plasma durations feature an increased CA of 130–140° owing to an increase in nanoscale roughness with plasma duration. In the case of AlOOH nanoflakes with three different Al coating thicknesses, all samples have higher CAs than those on the Si surfaces with nanopillars. The CAH is also lower on the hierarchically structured surfaces.

The nanopillar geometries on Si substrates varied in diameter and height with variation of the $CF_4$ plasma treatment duration. Theories of wetting behaviors on the micro-textured surfaces including Wenzel and Cassie–Baxter have been developed for single or dual micro/nano roughness scales.[26–28] The governing equations in these theories are derived from the interfacial energy minimization of single droplets on a textured surface. $\gamma_{LG}$ is the surface tension of the liquid–gas interface, $\gamma_{SL}$ is the surface tension of the solid–liquid interface, and $\gamma_{SG}$ is the surface tension of the solid–gas interface at equilibrium. Young's equation is given by $\cos\theta = (\gamma_{SG} - \gamma_{SL})/\gamma_{LG}$. In the Wenzel regime, a droplet is totally wetted on the surface and the apparent CA $\theta_W$ is given as a function of $r$ and $\theta$:

$$\cos\theta_W = r\cos\theta \tag{1}$$

Published on 08 August 2013. Downloaded by Korea Institute of Science and Technology / KIST on 02/10/2013 09:11:20.

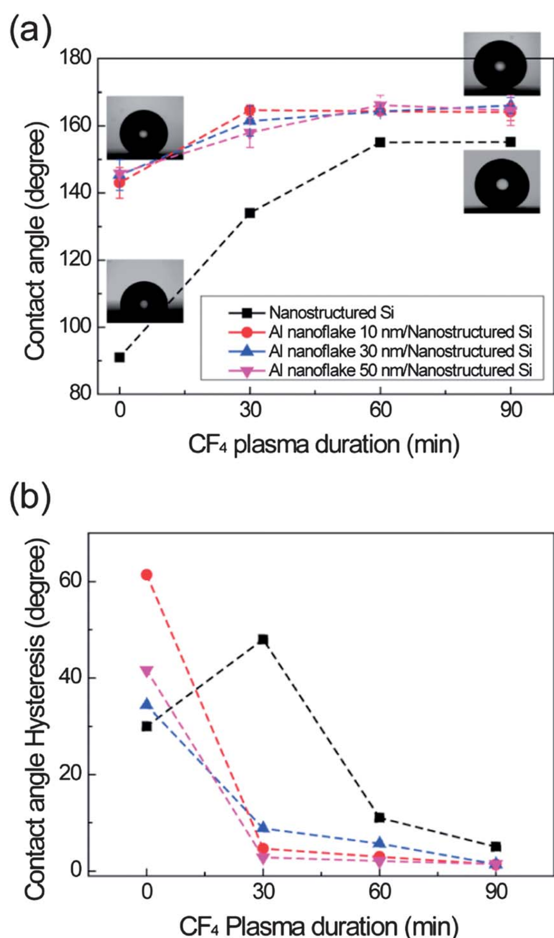


**Fig. 5** (a) CA and (b) CAH with respect to Al coating thickness on Si with nanopillars after hydrophobic coating. Some representative water droplets on the surfaces are present.

where $r$ is the dimensionless roughness, which is defined as a cylindrical pillar shape[29] and $\theta$ is the static CA on the flat surfaces. On the other hand, a droplet is suspended on the asperities of surfaces in the Cassie–Baxter regime and the apparent CA $\theta_{CB}$ is given as a function of $f_S$ and $\theta$:

$$\cos \theta_{CB} = f_S(\cos \theta + 1) - 1 \tag{2}$$

where $f_S$ is the solid fraction of contacted water in the pillar top area. As shown in Fig. 5b, the wetting behavior on Si surfaces with single roughness nanopillars received up to 30 min of $CF_4$ plasma treatment and could be described by the Wenzel state. The increases in CA and CAH were due to the nanostructure. However, the 60 and 90 min of $CF_4$ plasma treatment created a surface with a very low CAH of less than 10°, which is a characteristic of the Cassie–Baxter state. The water droplet maintains the superhydrophobic Cassie–Baxter state on the hierarchical surfaces composed of two different nanoscale roughnesses as shown in Fig. 1c. The surfaces with dual-scale roughness can be considered a nanoscale Cassie–Cassie (CC) state as discussed in prior studies.[27,28] The static CA on each state can be determined using Young's equation and energy minimization with the Cassie–Baxter equation considering nanopillars (P) and nanoflakes (F), which is given by

$$\cos \theta_{CC} = f_{SP} f_{SF}(\cos \theta + 1) - 1 \tag{3}$$

where the roughness factors $f_{SP}$ and $f_{SF}$ are calculated for nanopillars and nanoflakes, respectively, and by considering the nanostructures to be regular patterns. When the spacing between pillars and pillar diameter were 300 nm and 120 nm, respectively, the pillar height increased from 500 to 1500 nm for plasma durations from 30 to 90 min. Using these measurements, the theoretical CA is estimated at 143.8°, which is lower than the experimental measurement at approximately 150°. The pillar geometries were not uniform in height and width and the pillars randomly distributed, which is not reflected in the theory. In the case of AlOOH nanoflakes nested on Si nanopillars and a hierarchical structure having dual roughness, the CA is estimated at 163° and is derived from eqn (3) by taking a solid fraction of AlOOH nanoflakes as 0.01. The CA is calculated using a width of approximately 100 nm and a flake thickness of less than 50 nm. This result is quite similar to the values obtained by experiments (160–166°).

Along with superhydrophobicity, optical anti-reflectance is an essential requirement for the improvement of solar energy conversion in solar cells. In addition to improving hydrophobicity, controlled roughness plays a crucial role in reducing the light reflectance due to the enhancement of light scattering, which is similar to the moth-eye effect. In Fig. 6, optical images in visible color mode are compared to the surface roughness. As the Al thickness on the flat Si substrate increased, the surfaces turned blue, while on the nanopillared Si substrate without AlOOH nanoflakes, the surfaces turned dark. It can be considered that with the optical transparency of AlOOH of 95% above 350 nm in optical wavelength, optical absorption by the AlOOH layer increases on either flat or structured surfaces. In the case of hierarchical surfaces, as the Al thickness and $CF_4$ plasma

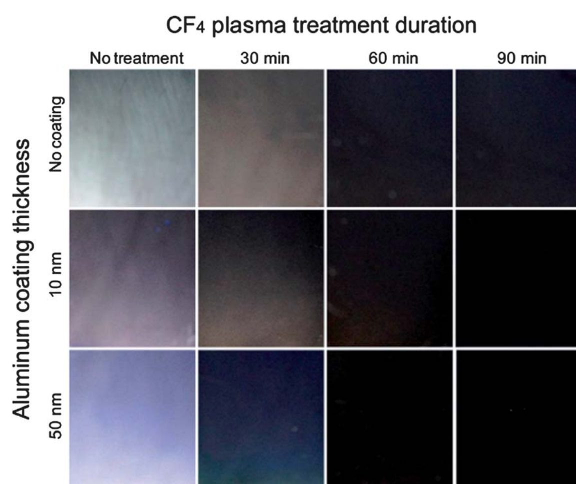


**Fig. 6** Optical images taken on various surfaces with increasing plasma etching duration from left to right, and with and without Al coating (10 nm and 50 nm thicknesses). The back plate is stainless steel. The view angle is 30°.

 This journal is © The Royal Society of Chemistry 2013

Published on 08 August 2013. Downloaded by Korea Institute of Science and Technology / KIST on 02/10/2013 09:11:20.

etching duration increased, the surface turned black due to incident light scattered by more complex geometries of AlOOH nanoflakes as shown in Fig. 2 and 3.

Fig. 7 shows the reflectance measured in the range of 200–2000 nm for pristine Si, single nanostructure of Si with nanopillars or AlOOH nanoflakes, and hierarchically nanostructured Si by the combination of AlOOH nanoflakes nested on nanopillars. In the case of the reflectance spectra of the flat single-roughness Si with AlOOH flakes, Fig. 7a indicates that as the Al coating thickness increased, the reflectance of Si gradually decreased to 11.9% for an incident light wavelength of 1200 nm, corresponding to the near-infrared region. This result is related to the covering density and the aspect ratio of hydroxide nanoflakes, which increased with the added Al coating thickness (Fig. 2). In Fig. 7b, a comparison of the reflectance spectra of Si before and after nanostructuring by $CF_4$ indicates a significant decrease in the reflectance of Si from 7.9 to 3.3% at a wavelength of 600 nm, corresponding to the visible region. This agrees well with the reflectance change on wet-etched Si reported in previous studies.[30,31] Compared to the reflectance reduction by AlOOH nanoflakes, the $CF_4$ plasma-etched Si pillars exhibited a greater improvement at a shorter wavelength regime of incident visible light. In Fig. 7c, nanoscale hierarchical structures with nanopillared Si using a fixed $CF_4$ etching duration of 60 min are shown to significantly reduce the reflectance to 4.1% for 600 nm light and 11.9% for 1200 nm light with the increase of Al thickness from 10 to 30 nm. Furthermore, the hierarchical structures with 90 min of $CF_4$ etching exhibited ultra-low reflectance (1.75%) at a wavelength of 600 nm and a reflectance of 8.2% at a wavelength of 1200 nm. The average reflectance value is measured for 200–2000 nm in optical wavelength on various substrates with flat single nanostructures and hierarchical nanostructures in Table 1.

The reflectance of flat Si having 35.8% would be reduced to 5.18% on the hierarchical nanostructure. Because Si with nanopillars having higher aspect ratios significantly reduced the reflectance, the effect of AlOOH nanoflakes is relatively lower in absolute value. Overall, the Si with nanopillars showed a higher reduction in reflectance for optical wavelengths below 600 nm, whereas the AlOOH flake acts on wavelengths above 600 nm. Therefore, the nanoscale combination of these two structures creates a hierarchical dual structure with improved anti-reflection over a wide range of visible wavelengths (Fig. 7c and d).

Density grading is enhanced with dual structures. Surfaces with only nanoscale pillars or only nanoflakes showed much higher reflectivity for visible wavelengths (Fig. 7a and b). Periodic grating structures can be analyzed using grating diffraction or the effective reflective index equation.[32,33] However, the anti-reflection characteristics of non-uniform dual structures are

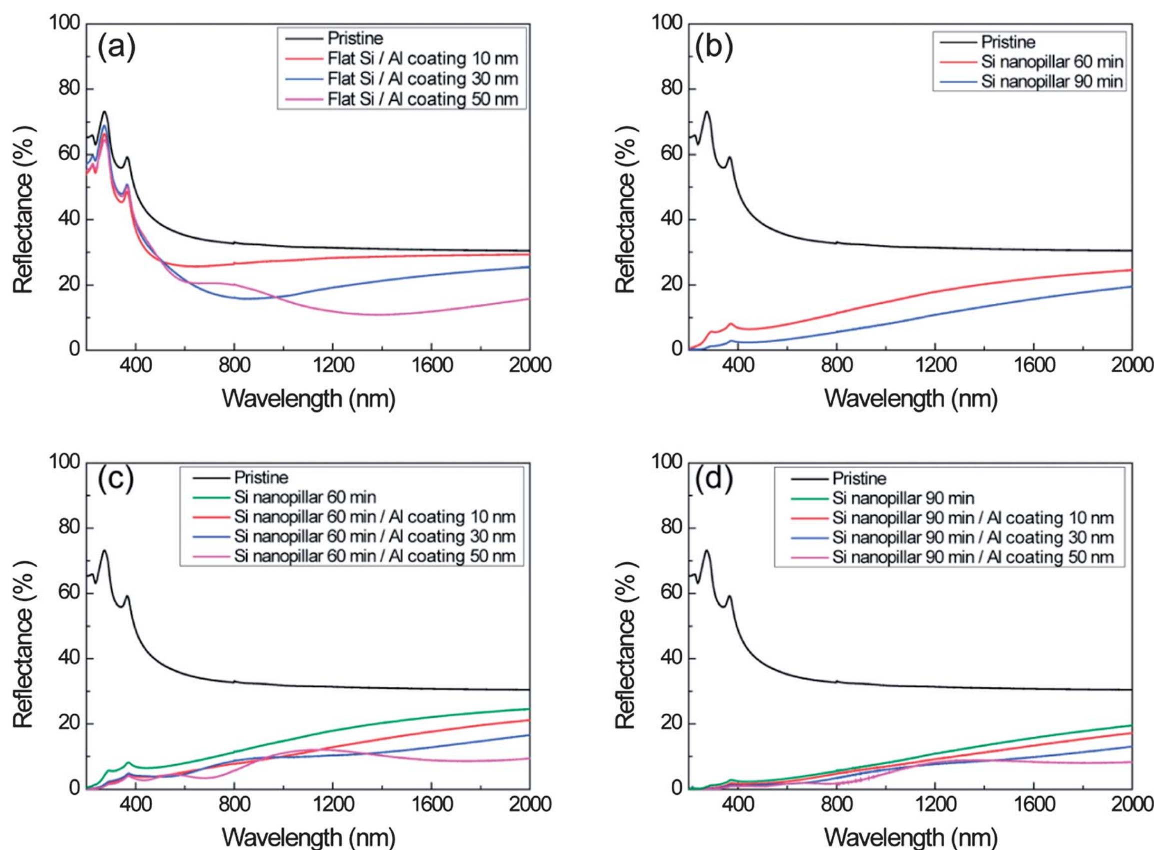


**Fig. 7** Reflectance is measured on various Si surfaces with a single roughness formed by (a) different $CF_4$ plasma treatment durations and (b) different Al coating conditions with water immersion. The reflectance is also evaluated on hierarchical structured surfaces with various Al coating thicknesses on nanopillar Si surfaces with plasma durations of (c) 60 min and (d) 90 min with respect to the incident light wavelength.

Published on 08 August 2013. Downloaded by Korea Institute of Science and Technology / KIST on 02/10/2013 09:11:20.

**Table 1** Reflectance (%) of various Si surfaces with respect to Si nanopillars or AlOOH nanoflakes

| Si structure | Al thickness (nm) | Wavelength (nm) 300 | 600 | 1200 | 1800 | Average |
|---|---|---|---|---|---|---|
| Pristine | 0 | 62.23 | 35.23 | 31.37 | 30.59 | 35.82 |
| | 10 | 53.26 | 25.80 | 28.25 | 29.16 | 30.81 |
| | 30 | 55.87 | 21.61 | 19.23 | 24.42 | 25.21 |
| | 50 | 53.96 | 21.09 | 11.93 | 13.73 | 20.39 |
| $CF_4$ 60 min | 0 | 5.56 | 7.95 | 17.90 | 23.48 | 15.32 |
| | 10 | 2.11 | 5.25 | 12.85 | 19.56 | 11.42 |
| | 30 | 2.53 | 4.67 | 10.30 | 14.69 | 9.41 |
| | 50 | 1.63 | 4.17 | 11.92 | 8.59 | 7.58 |
| $CF_4$ 90 min | 0 | 1.28 | 3.32 | 10.83 | 17.74 | 9.63 |
| | 10 | 0.52 | 2.45 | 9.18 | 15.33 | 8.14 |
| | 30 | 0.19 | 1.77 | 7.65 | 11.32 | 6.23 |
| | 50 | 0.11 | 1.75 | 8.17 | 8.01 | 5.18 |

difficult to analyze with Fresnel's equation or the diffraction grating equation due to the hierarchical structures with nanoscale roughness. Although the quantitative estimate of the effective reflective index for a dual density grading layer is not discussed in detail, it could be suggested that the dual structure with dual density graded layers provides a smoother continuous connection of the incident and passing media, lowering the reflectivity.

## 4 Conclusions

Anti-reflective and superhydrophobic surfaces having nanoscale hierarchical structures are introduced by the combination of AlOOH nanoflakes nested on plasma-etched Si nanopillars. AlOOH nanoflakes are formed by the Al thin film coating of different thicknesses and subsequent boiling water immersion *via* a bubble bursting mechanism on the Al oxide surface and the reaction of Al ions and water, confirming the boehmite phase by XRD and XPS. Hierarchical structures coated with a low surface energy material have higher water CA (over 150°), while the contact angle hysteresis is very low, implying the creation of a self-cleaning surface with a dual-scale Cassie–Cassie mode. Reflectance is significantly reduced to 5.18% on average by the presence of hierarchical nanostructures that are enhanced by the combination of two different surface textures on the nanoscale: Si nanopillars with higher aspect ratios for higher reduction in reflectance for optical wavelengths from 200 to 1200 nm and AlOOH nanoflakes for optical wavelengths above 600 nm. Using the synergetic effect of the dual nanostructures, which exhibit ultra-low reflectance as well as superhydrophobicity, the hierarchical surfaces can be used for solar cell panels or some display devices to increase performance and improve durability through self-cleaning under harsh environments.

## Acknowledgements

This work was supported by a KIST internal project, the Global Excellent Technology Innovation R&D Program, by the Ministry of Knowledge Economy (MKE) of the Republic of Korea and project no. 10040003, funded by the MKE. This work was also funded by the Ministry of Education, Science, and Technology (R11-2005-065, OKH).

## References

1 J. Zhu, C.-M. Hsu, Z. Yu, S. Fan and Y. Cui, *Nano Lett.*, 2010, **10**, 1979.
2 K. Forberich, G. Dennler, M. C. Scharber, K. Hingerl, T. Fromherz and C. J. Brabec, *Thin Solid Films*, 2008, **516**, 7167.
3 M. Srinivasarao, *Chem. Rev.*, 1999, **99**, 1935.
4 W. H. Miller, G. D. Bernard and J. L. Allen, *Science*, 1968, **162**, 760.
5 P. Vukusic and J. R. Sambles, *Nature*, 2003, **424**, 852.
6 S. Chattopadhyay, Y. F. Huang, Y. J. Jen, A. Ganguly, K. H. Chen and L. C. Chen, *Mater. Sci. Eng., R*, 2010, **69**, 1.
7 Y. Li, J. Zhang and B. Yang, *Nano Today*, 2010, **5**, 117.
8 E. K. Her, T.-J. Ko, K.-R. Lee, K. H. Oh and M.-W. Moon, *Nanoscale*, 2012, **4**, 2900.
9 S.-Y. Han, B. K. Paul and C.-h. Chang, *J. Mater. Chem.*, 2012, **22**, 22906.
10 G. S. Watson and J. A. Watson, *Appl. Surf. Sci.*, 2004, **235**, 139.
11 T. L. Sun, L. Feng, X. F. Gao and L. Jiang, *Acc. Chem. Res.*, 2005, **38**, 644.
12 D. Quere, *Annu. Rev. Mater. Res.*, 2008, **38**, 71.
13 W. Barthlott and C. Neinhuis, *Planta*, 1997, **202**, 1.
14 J. Zhang, S. Liu, J. Lin, H. Song, J. Luo, E. M. Elssfah, E. Ammar, Y. Huang, X. Ding, J. Gao, S. Qi and C. Tang, *J. Phys. Chem. B*, 2006, **110**, 14249.
15 S.-C. Cha, E. K. Her, T.-J. Ko, S. J. Kim, H. Roh, K.-R. Lee, K. H. Oh and M.-W. Moon, *J. Colloid Interface Sci.*, 2013, **391**, 152.
16 T. Y. Kim, B. Ingmar, K. Bewilogua, K. H. Oh and K.-R. Lee, *Chem. Phys. Lett.*, 2007, **436**, 199.
17 M. Grischke, A. Hieke, F. Morgenweck and H. Dimigen, *Diamond Relat. Mater.*, 1998, **7**, 454.
18 K. Tadanaga, N. Katata and T. Minami, *J. Am. Ceram. Soc.*, 1997, **80**, 3213.
19 J. Yang, Z. Zhang, X. Men, X. Xu, X. Zhu, X. Zhou and Q. Xuea, *J. Colloid Interface Sci.*, 2012, **366**, 191.
20 R. Tettenhorst and D. A. Hofmann, *Clays Clay Miner.*, 1980, **28**, 373.
21 J. T. Kloprogge, L. V. Duong, B. J. Wood and R. L. Frost, *J. Colloid Interface Sci.*, 2006, **296**, 572.
22 R. K. Hart, *Trans. Faraday Soc.*, 1957, **53**, 1020.
23 R. K. Hart, *Trans. Faraday Soc.*, 1954, **50**, 269.
24 M. He, X. Zhou, X. Zeng, D. Cui, Q. Zhang, J. Chen, H. Li, J. Wang, Z. Cao, Y. Song and L. Jiang, *Soft Matter*, 2012, **8**, 6680.
25 A. Hozumi, B. Kim and T. J. McCarthy, *Langmuir*, 2009, **25**, 6834.
26 A. W. Adamson, *Physical Chemistry of Surfaces*, John Wiley & Sons, New York, 5th edn, 1990, ch. X, Section 4.
27 Y. Rahmawan, M.-W. Moon, K.-S. Kim, K.-R. Lee and K.-Y. Suh, *Langmuir*, 2010, **26**, 484.

 This journal is © The Royal Society of Chemistry 2013

28 T.-G. Cha, J. W. Yi, M.-W. Moon, K.-R. Lee and H.-Y. Kim, *Langmuir*, 2010, **26**, 8319.
29 C.-H. Choi and C.-J. Kim, *Phys. Rev. Lett.*, 2006, **96**, 066001.
30 J. S. Yoo, I. O. Parm, U. Gangopadhyay, K. Kim, S. K. Dhungel, D. Mangalaraj and J. Yi, *Sol. Energy Mater. Sol. Cells*, 2006, **90**, 3085.
31 H. M. Branz, V. E. Yost, S. Ward, K. M. Jones, B. To and P. Stradins, *Appl. Phys. Lett.*, 2009, **94**, 231121.
32 Y. M. Song, E. S. Choi, G. C. Park, C. Y. Park, S. J. Jang and Y. T. Lee, *Appl. Phys. Lett.*, 2010, **97**, 093110.
33 E. K. Her, T. J. Ko, B. Shin, H. Roh, W. Dai, W. K. Seong, H.-Y. Kim, K.-R. Lee, K. H. Oh and M.-W. Moon, *Plasma Process. Polym.*, 2013, **10**, 401.

Published on 08 August 2013. Downloaded by Korea Institute of Science and Technology / KIST on 02/10/2013 09:11:20.